

A Review of Image Processing Methods and Biometric Trends for Personal Authentication and Identification

Ryszard S. Choras

Institute of Telecommunications and Computer Sciences;
UTP University of Science and Technology;
85-796 Bydgoszcz, S. Kaliskiego 7, Poland;
e-mail:choras@utp.edu.pl

Abstract—This paper is a survey on methods of image processing and recognition for human identification. Image processing system is defined and different types of features are extracted from a user. A biometric system is a pattern recognition system that recognizes a person based on a feature vector derived from a specific physiological or behavioral characteristic that the person possesses. Biometric system may be viewed as a pattern recognition system that extracts a set of discriminative features from the input biometric template. Since traditional biometric systems have many limitations a new approach in biometrics used different models of multimodal systems. In multimodal biometric system various levels of fusion the personal attributes information is performed. We discuss model of soft biometric features and methods and techniques for automated recognition based on those characteristics. We consider the current technical issues and challenges regarding the use of biometric system.

I. INTRODUCTION

The term digital image processing generally refers to processing of a two-dimensional picture by a digital computer [2]. The discussion of the image processing algorithms should be divided in four major groups [11]:

- image capture,
- image preprocessing,
- feature extraction,
- pattern recognition.

The pictorial information is represented as a function of two variables (x, y) . The image in its digital form is usually stored as a two-dimensional array. If $M = \{1, 2, \dots, x, \dots, m\}$ and $N = \{1, 2, \dots, y, \dots, n\}$ are the spatial domain, then $D = M \times N$ is the set of resolution cells and the digital image I is a function which assigns some greytone value $G \in \{0, 1, \dots, 2^{r-1}\}$ to each and every resolution cell, i.e. $I = M \times N \rightarrow G$. Formally

$$D = \{(x, y) | x \in M, y \in N\} \quad (1)$$

and

$$I = \{I(x, y) | (x, y) \in D \text{ and } I(x, y) \in 0, 1, \dots, 2^{r-1}\} \quad (2)$$

The basic idea of the image processing system is presented in (Fig. 1).

Image processing system in the preprocessing stage is first processed in order to extract the features. The processing

involves filtering, normalization, segmentation, and object identification. The output of this stage is a set of significant regions and objects.

In the feature extraction stage, feature extraction algorithm produces a feature vector, in which the components are numerical characterizations of the parts.

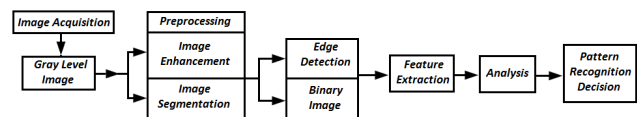


Fig. 1. Schematic diagram of the image processing system.

Features should be extracted automatically from the images. Automatic extraction can be used only for the most primitive features, like color (computing the average color, the color histogram or color covariances of an area of the image) or size of a region of the image.

Feature extraction is the process of generating features to be used in the selection and classification tasks. Feature selection reduces the number of features provided to the classification task. Those features which are likely to assist in discrimination are selected and used in the classification task. Features which are not selected are discarded.

We classify the various features currently employed as follows:

- General features: Application independent features such as color, texture, and shape. According to the abstraction level, they can be further divided into:
 - Pixel-level features: Features calculated at each pixel, e.g. color, location.
 - Local features: Features calculated over the results of subdivision of the image band on image segmentation or edge detection.
 - Global features: Features calculated over the entire image or just regular sub-area of an image.
- Domain-specific features: Application dependent features such as human faces, fingerprints, and conceptual features. These features are often a synthesis of low-level features for a specific domain.

On the other hand, all features can be coarsely classified into low-level features and high-level features. Low-level features can be extracted directly from the original images, whereas high-level feature extraction must be based on low-level features.

II. BIOMETRIC SYSTEM

All biometric systems work in a similar fashion:

- 1) The user submits a sample that is an identifiable, unprocessed image or recording of the physiological or behavioral biometric via an acquisition device,
- 2) This image and/or biometric is processed to extract information about distinctive features.

Biometric systems have four main components [18]: sensor, feature extraction, biometric database, matching-score and decision-making modules (Fig. 2). The input subsystem consists of a special sensor needed to acquire the biometric signal. Invariant features are extracted from the signal for representation purposes in the feature extraction subsystem. During the enrollment process, a representation (called template) of the biometrics in terms of these features is stored in the system. The matching subsystem accepts query and reference templates and returns the degree of match or mismatch as a score, i.e., a similarity measure. A final decision step compares the score to a decision threshold to deem the comparison a match or non-match.

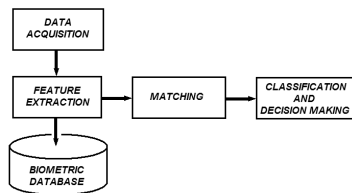


Fig. 2. Biometric system as a pattern recognition system

The ideal biometric characteristics have following qualities:

- Robust: Unchanging on an individual over time. "Robustness" is measured by the probability that a submitted sample will not match the enrollment image.
- Universality: Every person should have the biometric characteristic.
- Distinctive: Showing great variation over the population. "Distinctiveness" is measured by the probability that a submitted sample will match the enrollment image of another user.
- Uniqueness: No two persons should be the same in terms of the biometric characteristic.
- Available: The entire population should ideally have this measure in multiples. "Availability" is measured by the probability that a user will not be able to supply a readable measure to the system upon enrollment.
- Permanence: The biometric characteristic should be invariant over time.

- Collectability: The biometric characteristic should be measurable with some (practical) sensing device.
- Accessible: Easy to image using electronic sensors. "Accessibility" can be quantified by the number of individuals that can be processed in a unit time, such as a minute or an hour.
- Acceptable: People do not object to having this measurement taken on them. "Acceptability" is measured by polling the device users. One would want to minimize the objections of the users to the measuring/collection of the biometric.

A biometric system is a pattern recognition system that recognizes a person on the basis of a feature vector derived from a specific physiological or behavioral characteristic that the person possesses [19]. Physiological Biometrics - also known as static biometrics - based on data derived from the measurement of a part of a person's anatomy. For example, fingerprints and iris patterns, as well as facial features, hand geometry and retinal blood vessels. Behavioral biometrics based on data derived from measurement of an action performed by a person and, distinctively, incorporating time as a metric, that is, the measured action. The behavioral characteristics measure the movement of a user, when users walk, speak, type on a keyboard or sign their name.

Invariant features are extracted from the signal for representation purposes in the feature extraction subsystem. During the enrollment process, a representation (called template) of the biometrics in terms of these features is stored in the system. The matching subsystem accepts query and reference templates and returns the degree of match or mismatch as a score, i.e., a similarity measure. A final decision step compares the score to a decision threshold to deem the comparison a match or non-match. The personal attributes used in a biometric identification system can be physiological, such as facial features, fingerprints, iris, retinal scans, hand and finger geometry; or behavioral, the traits idiosyncratic of the individual, such as voice print, gait, signature, and keystroking.

A generalized diagram of a biometric system is shown in Figure 3. The component which is of great importance is the feature extraction algorithm. Feature extraction algorithm produces a feature vector, in which the components are numerical characterizations of the underlying biometrics.

The feature vectors are designed to characterize the underlying biometrics so that biometric data collected from one individual, at different times, are "similar", while those collected from different individuals are "dissimilar". In general, the larger the size of a feature vector (without much redundancy), the higher its discrimination power. The discrimination power is the difference between a pair of feature vectors representing two different individuals. The next component of the system is the "matcher", which compares feature vectors obtained from the feature extraction algorithm to produce a similarity score. This score indicates the degree of similarity between a pair of biometrics data under consideration.

The problem of resolving the identity of a person can be categorized into two fundamentally distinct types of problems with different inherent complexities:

(i) verification (also called authentication) refers to the problem of confirming or denying a person's claimed identity (Am I who I claim to be?) (Fig. 4). In a process of verification (1-to-1 comparison), the biometrics information of an individual, who claims certain identity, is compared with the biometrics on the record that represent the identity that this individual claims. The comparison result determines whether the identity claims shall be accepted or rejected. Given the input x that claims to belong to the class y_k , we need to verify whether this is true. The answer a is a binary *yes* or *no* :

$$a = \begin{cases} \text{yes} & \text{if } f(x, y_k) \leq T \\ \text{no} & \text{otherwise} \end{cases} \quad (3)$$

where T is a given threshold.

and

(ii) identification (Who am I?) refers to the problem of establishing a subject's identity (Fig. 5). It is often desirable to be able to discover the origin of certain biometrics information to prove or disprove the association of that information with a certain individual. This process is commonly known as identification (1-to-many comparison). Given p image-class templates y_i $i = 1, \dots, p$, that correspond to p individuals stored in a database, we need to find the closest match to our input x as follows:

$$\hat{y} = y_k \quad \text{if } f(x, y_k) = \min_{y_i} f(x, y_i) \quad (4)$$

where $f(x, y)$ is a suitably chosen cost function that is dependent on the application.

Verification systems are more accurate, less expensive and faster than Identification systems. However, their drawbacks are: they are more limited in function, and they require a lot more effort from the user, to use the system.

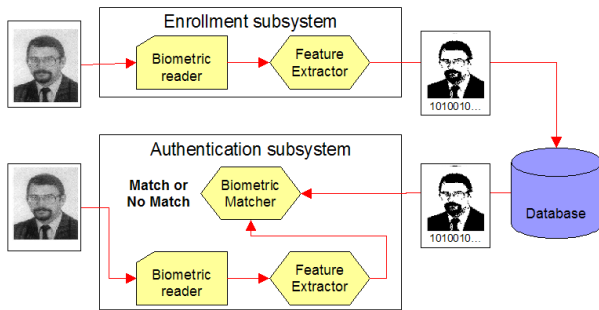


Fig. 3. Biometric system

In this paper a recognition methods are presented for recognizes a person on the basis of a feature vector derived from biometrics templates (images).

III. FEATURE EXTRACTION BASED ON TEXTURE

Texture is a powerful regional descriptor that helps in the retrieval process. Texture, on its own does not have the

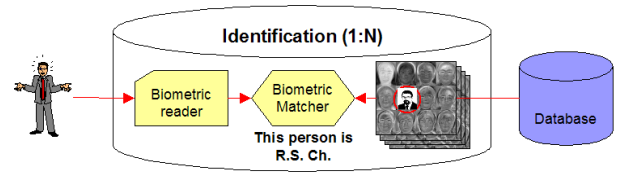


Fig. 4. Identification process

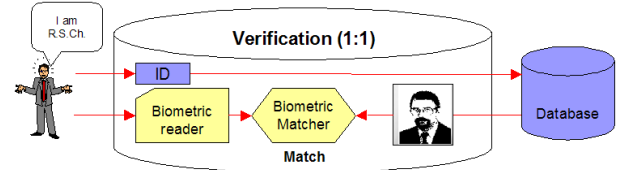


Fig. 5. Verification process

capability of finding similar images, but it can be used to classify textured images from non-textured ones and then be combined with another visual attribute like color to make the retrieval more effective.

One of the popular representations of texture feature is the co-occurrence matrix proposed by Haralick et al. [14], [15]. The matrix is based on pixel orientation and inter-pixel distance. Meaningful statistics from the co-occurrence matrix are extracted and represented as texture information.

The co-occurrence matrix $C(i, j)$ counts the co-occurrence of pixels with gray values i and j at a given distance d . The distance d is defined in polar coordinates (d, α) , with discrete length and orientation. In practice, α takes the values 0° ; 45° ; 90° ; 135° ; 180° ; 225° ; 270° ; and 315° . The co-occurrence matrix $C(i, j)$ can now be defined as follows:

$$C(i, j) = Pr(I(p_1) = i \wedge I(p_2) = j \mid |p_1 - p_2| = d) \quad (5)$$

where Pr is probability, and p_1 and p_2 are positions in the gray-scale image I .

Texture features which can be extracted from gray level co-occurrence matrices are as follows:

Angular Second Moments

$$\sum_i \sum_j C(i, j)^2 \quad (6)$$

Correlation

$$\frac{\sum_i \sum_j (ij)C(i, j) - \mu_i \mu_j}{\sigma_i \sigma_j} \quad (7)$$

Variance

$$\sum_i \sum_j (i - j)^2 C(i, j) \quad (8)$$

Inverse Difference Moment

$$\sum_i \sum_j \frac{1}{1 + (i - j)^2} C(i, j) \quad (9)$$

Entropy

$$-\sum_i \sum_j C(i, j) \log C(i, j) \quad (10)$$

TABLE I
PHYSIOLOGICAL BIOMETRIC MODALITIES

Biometric modalities	Description	References
Face	Face recognition systems typically utilize the spatial relationship among the locations of facial features such as eyes, nose, lips, chin, and the global appearance of a face. Face recognition is non-intrusive, has high user acceptance, and provides acceptable levels of recognition performance in controlled environments.	[1], [19], [24], [44], [52]
Fingerprint	Fingerprint-based recognition is most successful and popular method for person identification. Fingerprints consist of a regular texture pattern composed of ridges and valleys. These ridges are characterized by several landmark points, known as minutiae, which are mostly in the form of ridge endings and ridge bifurcations. The spatial distribution of these minutiae points is claimed to be unique to each finger.	[3], [16], [23], [41], [47], [47]
Iris	The iris is a protected internal organ whose texture pattern with numerous individual attributes, e.g. stripes, pits, and furrows, is stable and distinctive, even among identical twins. According to the various iris features utilized, iris recognition algorithms can be grouped into four main categories: <ol style="list-style-type: none"> 1) Phase-based method. Daugman extracted the phase measures as the iris feature. The phase is coarsely quantized to four values and the iris code is 256 bytes long. Then the dissimilarity between the input iris image and the registered template can be easily determined by the Hamming distance between their IrisCodes. 2) Zero-crossings representation. 3) Texture analysis. Naturally, random iris pattern can be seen as texture, so many well-developed texture analysis methods can be adapted to recognize the iris. Gabor filters are used to extract the iris features. 4) Local intensity variation. 	[3], [4], [7], [8], [11], [17], [26]–[29], [33], [35], [35], [37], [40], [42], [43]
Palmprint	The image of a human palm consists of palmar friction ridges similar to fingerprints. These systems utilize texture features which are quite similar to those employed for iris recognition.	[22], [51]
Hand Geometry	The hand geometry utilizes hand images to extract a number of geometrical features such as finger length, width, thickness, perimeter and finger area.	[12]
Ear	The shape of the outer ear has long been recognized as a valuable means for personal identification. There are two major subfields ear biometrics: 2D ear recognition and 3D ear recognition. Some of different ear recognition methods are: Force Field Transformation, 2D and 3D ear shape descriptors, "Eigen-Ear", Principal Component Analysis (PCA), Moment invariants. Ear does not change during human life.	[2], [2], [5], [21]
Periocular	The periocular region represents the region around the eyes. The periocular region (region around the eye) may be useful as a soft biometric. Features of the periocular region, can be divided into two levels: <ul style="list-style-type: none"> - the first level comprise the eyelids, eye folds, and eye corners; - second level comprises the skin texture, wrinkles, color and pores. In periocular biometric recognition, as features were used local descriptors as LBP (Local Binary Pattern), HOG (Histogram of Oriented Gradients) and global descriptor SIFT (Shift Invariant Feature Transform). Analysis of those features can be carried on based on their geometry, texture or color.	[32], [36], [45]
Retina	Retina scan is based on the blood vessel pattern in the retina of the eye. The blood vessel is distinctive pattern for each retina of the person. Retinal scan captures the pattern of eyes blood vessels. Pattern of retina's blood vessels rarely changes during people's lives. The feature vector have small size.	[6], [30]
Hand vein. Finger vein. Forearm vein.	Hand vein geometry is based on the fact that the vein pattern is distinctive for various individuals. The current available approaches for finger vein recognition are all based on texture extraction based on one single infrared image of finger vein. The minutiae features include bifurcation points and ending points are extracted from vein patterns. These feature points are used for geometric representation of the vein patterns shape.	[36], [46], [49], [50]

Inertia (or contrast)

$$\sum_i \sum_j (i-j)^2 C(i,j) \quad (11)$$

Cluster Shade

$$\sum_i \sum_j ((i-\mu_i) + (j-\mu_j))^3 C(i,j) \quad (12)$$

Statistical methods, including multi-resolution filtering techniques such as Gabor and wavelet transform, characterize texture by the statistical distribution of the image intensity. Motivated by biological findings on the similarity of two-dimensional (2D) Gabor filters there has been increased interest in deploying Gabor filters in various computer vision applications.

The general functionality of the 2D Gabor filter family can be represented as a Gaussian function modulated by a complex sinusoidal signal. Specially, a 2D Gabor filter $g(x, y)$ can be formulated as

$$g(x, y; F, \theta) = \frac{1}{2\pi\sigma_x\sigma_y} \exp\left[-\frac{1}{2}\left(\frac{\bar{x}^2}{\sigma_x^2} + \frac{\bar{y}^2}{\sigma_y^2}\right)\right] \exp[2\pi j F \bar{x}] \quad (13)$$

where

$$\begin{bmatrix} \bar{x} \\ \bar{y} \end{bmatrix} = \begin{bmatrix} \cos\theta & \sin\theta \\ -\sin\theta & \cos\theta \end{bmatrix} \cdot \begin{bmatrix} x \\ y \end{bmatrix}, \quad j = \sqrt{-1}$$

and

- σ_x and σ_y are the scaling parameters of the filter and determine the effective size of the neighborhood of a pixel in which the weighted summation (convolution) takes place,
- θ ($\theta \in [0, \pi]$) specifies the orientation of the Gabor filters,
- F is the radial frequency of the sinusoid.

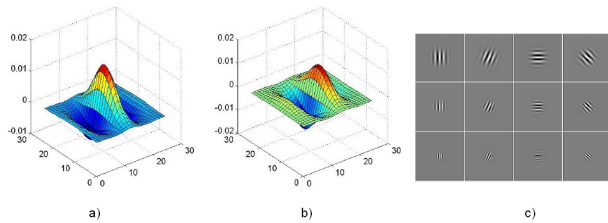


Fig. 6. Real (a) and imaginary (b) parts of Gabor wavelets and Gabor kernels with different orientations (c)

Gabor filters worked as local bandpass filters and each filter is fully determined by choosing the four parameters $\{\theta, F, \sigma_x, \sigma_y\}$. Assuming that N filters are needed in an application, $4N$ parameters need to be optimized. The orientation parameter θ should satisfy $\theta \in [0, \pi]$. W is the radial frequency of the Gabor filter and is application dependent. σ_x and σ_y are the effective sizes of the Gaussian functions and are within the range $[\sigma_{min}, \sigma_{max}]$.

The Gabor filter $g(x, y; F, \theta)$ forms complex valued function. Decomposing $g(x, y; F, \theta)$ into real and imaginary parts gives

$$g(x, y; F, \theta) = r(x, y; F, \theta) + ji(x, y; F, \theta) \quad (14)$$

where

$$\begin{aligned} r(x, y; F, \theta) &= g(x, y; F, \theta) \cos(2\pi F, \bar{x}) \\ i(x, y; F, \theta) &= g(x, y; F, \theta) \sin(2\pi F, \bar{x}) \end{aligned} \quad (15)$$

The Gabor filtered output of an image $I(x, y)$ is obtained by the convolution of the image with the Gabor function $g(x, y; F, \theta)$. Given a neighborhood window of size $W \times W$ for $W = 2t + 1$, the discrete convolutions of $I(x, y)$ with respective real and imaginary components of $g(x, y; F, \theta)$ are

$$C_{ev}(x, y; F, \theta) = \sum_{l=-t}^t \sum_{m=-t}^t I(x+l, y+m) r(x, y; F, \theta) \quad (16)$$

$$C_{odd}(x, y; F, \theta) = \sum_{l=-t}^t \sum_{m=-t}^t I(x+l, y+m) i(x, y; F, \theta) \quad (17)$$

The channel output is computed as

$$C(x, y; F, \theta) = \sqrt{(C_{ev}(x, y; F, \theta))^2 + (C_{odd}(x, y; F, \theta))^2} \quad (18)$$

After applying Gabor filters on the image with different scale s and orientation k we obtain an array of magnitudes. These magnitudes represent the energy content at different scale and orientation of the image.

The following mean μ_{sk} and standard deviation S_{sk} of the magnitude of the transformed coefficients are used to represent the homogenous texture feature of the region

$$\mu_{sk} = \frac{1}{MN} \sum_{x=1}^M \sum_{y=1}^N C_{sk}(x, y; F, \theta) \quad (19)$$

$$S_{sk} = \sqrt{\sum_{x=1}^M \sum_{y=1}^N (C_{sk}(x, y; F, \theta) - \mu_{sk})^2} \quad (20)$$

where $s = 0, 1, \dots, S-1$ and $k = 0, \dots, K-1$.

The feature vector (FV) is constructed using μ_{sk} and S_{sk} as feature components.

IV. OCULAR BIOMETRICS - AUTOMATIC FEATURE EXTRACTION FROM EYE IMAGES

A. Iris recognition

Iris texture patterns are believed to be different for each person, and even for the two eyes of the same person. It is also claimed that for a given person, the iris patterns change little after youth.

The iris (see Fig.7) is the colored portion of the eye that surrounds the pupil. Its combination of pits, striations, filaments, rings, dark spots and freckles make for a very accurate means of biometric identification [7], [11]. Its

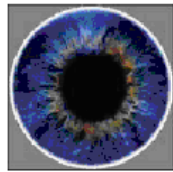


Fig. 7. The iris

uniqueness is such that even the left and right eye of the same individual is very different.

A major approach for iris recognition today is to generate feature vectors corresponding to individual iris images and to perform iris matching based on some distance metrics [3], [4], [42], [43].

The initial stage deals with iris segmentation. This consists in localizing the iris inner (pupillary) and outer (scleric) borders. In order to compensate the varying size of the captured iris it is common to translate the segmented iris region, represented in the cartesian coordinate system, to a fixed length and dimensionless polar coordinate system. The next stage is the feature extraction. In the final stage it is made a comparison between iris features, producing a numeric dissimilarity value.

Robust representations for iris recognition must be invariant to changes in the size, position and orientation of the patterns. This means that a representation of the iris data invariant to changes in the distance between the eye and the capturing device, in the camera optical magnification factor and in the iris orientation. As described in [11], the invariance to all of these factors can be achieved by the translation of the captured data to a double dimensionless pseudo-polar coordinate system.

Formally, to each pixel of the iris, regardless its size and pupillary dilation, a pair of real coordinates (r, θ) , where r is on the unit interval $[0, 1]$ and θ is an angle in $[0, 2\pi]$. The remapping of the iris image $I(x, y)$ from raw cartesian coordinates (x, y) to the dimensionless non concentric polar coordinate system (r, θ) can be represented as:

$$I(x(r, \theta), y(r, \theta)) \rightarrow I(r, \theta) \quad (21)$$

where $x(r, \theta)$ and $y(r, \theta)$ are defined as linear combinations of both the set of pupillary boundary points $(x_p(\theta), y_p(\theta))$ and the set of limbus boundary points along the outer perimeter of the iris $(x_s(\theta), y_s(\theta))$ bordering the sclera:

$$\begin{aligned} x(r, \theta) &= (1 - r) \cdot x_p(\theta) + r \cdot x_s(\theta) \\ y(r, \theta) &= (1 - r) \cdot y_p(\theta) + r \cdot y_s(\theta) \end{aligned} \quad (22)$$

Iris edge point detection means to find some points on the inner and outer boundary of iris. We should find out the coarse center of the pupil in the binary image. As we know, the intensity value of the pupil region is the lowest in the whole image. We can use the equation below to detect the coarse center of the pupil from the binary image.

The remapping is done so that the transformed image is rectangle with some dimension, typically as in [11] 48×448 (Fig. 8).

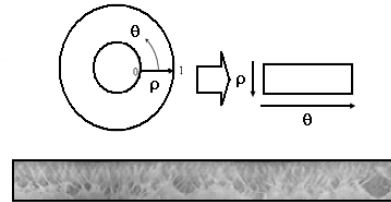


Fig. 8. Transformed region

Because most of the irises are affected by upper and lower eyelids, the iris is divided into two rectangular (Fig. 9a) or two angular sectors (Fig. 9b) having the same size. The blocks of interest (ROI) should be isolated from the normalized iris image.

Most of iris recognition systems are based on Gabor functions analysis in order to extract iris image features. It consists in convolution of image with complex Gabor filters which is used to extract iris feature. As a product of this operation, complex coefficients are computed. In order to obtain iris signature, complex coefficients are evaluated and coded.

The normalized iris images (Fig. 8) are divided into two stripes, and each stripe into $K \times L$ blocks. The size of each block is $k \times l$. Localization of blocks is shown in Fig. 10. Each block is filtered by

$$Gab(x, y, \alpha) = \sum_{x-\frac{k}{2}}^{x+\frac{k}{2}} \sum_{y-\frac{l}{2}}^{y+\frac{l}{2}} I(x, y) \cdot g(x, y) \quad (23)$$

The orientation angles of this set of Gabor filters are

$$\langle \alpha_i | \alpha_i = \frac{i\pi}{4}, \quad i = 0, 1, 2, 3 \rangle \quad (24)$$

To encode the iris we used the real part of (23) as

$$\begin{aligned} Code(x, y) &= 1 \quad \text{if } Re(Gab(x, y, \alpha_i)) \geq th \\ Code(x, y) &= 0 \quad \text{if } Re(Gab(x, y, \alpha_i)) < th \end{aligned} \quad (25)$$

The iris binary *Code* can be stored as personal identify feature.

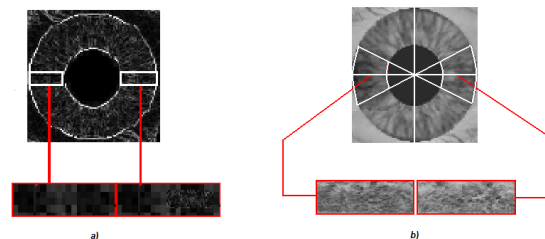


Fig. 9. The iris ROI

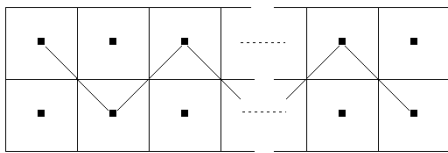


Fig. 10. Localization of blocks.

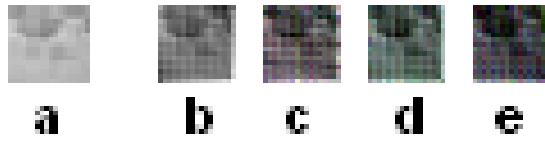


Fig. 11. Original block iris image (a) and real part of $Gab(x, y, \alpha_i)$ for $\alpha_i = 0^\circ$ (b), $\alpha_i = 45^\circ$ (c), $\alpha_i = 90^\circ$ (d), $\alpha_i = 135^\circ$ (e)

B. Retina and Conjunctiva Biometrics

The retina is a thin layer of cells at the back of the eyeball of vertebrates. It is the part of the eye which converts light into nervous signals. It is lined with special photoreceptors which translate light into signals to the brain. Every eye has its own totally unique pattern of blood vessels. The unique structure of the blood vessels in the retina has been used for biometric identification.

The conjunctiva is a thin, clear, highly vascular and moist tissue that covers the outer surface of the eye (sclera). Conjunctival vessels can be observed on the visible part of the sclera.

In computer diagnosis of eye diseases several features of retinal/conjunctival vessels as diameter, length, branching angle can be used.

Vessel pattern is unique for each human being even in the case of identical twins. Moreover, it is a highly stable pattern over time. Scanning is performed using a low-intensity light source and an optical coupler to scan the unique patterns and it does require the user to remove glasses, place their eye close to the device, and focus on a certain point. The acquisition process requires collaboration from the user and it is sometimes perceived as intrusive.

The five main stages in the feature point extraction process are:

- 1) Image retina/conjunctiva acquisition,
- 2) Image preprocessing (color transformation, edge detection, etc.),
- 3) Extraction of geometrical features,
- 4) Extraction of texture features,
- 5) Integration of geometrical and texture features.

Images which are considered in this paper as Retina-1 and Conjunctiva-1, are displayed in Figure 13.

1) *Preprocessing*: Before performing feature extraction, the original eye images are subjected to some image processing operations, as:

- 1) Color transformation. To represent eye characteristic we using luminance component (Y) from YC_bC_r (YIQ)



Fig. 12. Iris Code

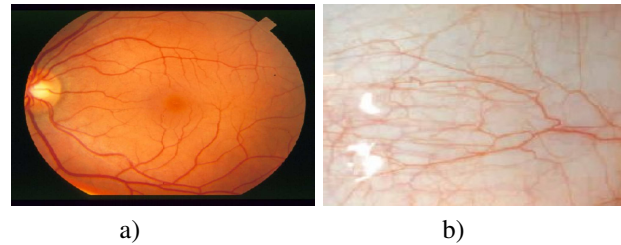


Fig. 13. Retina-1 (a) and Conjunctiva-1 (b) images.

color space (Fig 2).

$$\begin{bmatrix} Y \\ C_r \\ C_b \end{bmatrix} = \begin{bmatrix} 0,299 & 0,587 & 0,114 \\ 0,500 & -0,419 & -0,081 \\ -0,169 & -0,331 & 0,500 \end{bmatrix} \begin{bmatrix} R \\ G \\ B \end{bmatrix} \quad (26)$$

- 2) Image stretched. The contrast level is stretched according to

$$I_{out}(x, y) = 255 \times \left(\frac{I_{in}(x, y) - \min}{\max - \min} \right)^\gamma \quad (27)$$

$I_{out}(x, y)$ is the color level for the output pixel (x, y) after the contrast stretching process. $I_{in}(x, y)$ is the color level input for data the pixel (x, y) . \max - is the maximum value for color level in the input image. \min - is the minimum value for color level in the input image, γ - constant that defines the shape of the stretching curve.

- 3) Noise elimination. Noise pixels add irregularities to the outer boundary of the vessels and may have undesired effects on the recognition system. The algorithm modifies each pixel according to its initial value and to those of its neighborhood according to the following conditions:

$$\text{If } p = 1 \text{ then } p' = \begin{cases} 0 & \text{if } \sum_{i=1}^8 p_i \leq T_1 \\ 1 & \text{otherwise} \end{cases}$$

$$\text{else } p' = \begin{cases} 1 & \text{if } \sum_{i=1}^8 p_i > T_2 \\ 0 & \text{otherwise} \end{cases} \quad (28)$$

where p is current pixel value, p' the new pixel value and and T_1 are T_2 the threshold values.

p_4	p_3	p_2
p_5	p	p_1
p_6	p_7	p_8

Fig. 14. Pixel notations

- 4) Edge detection. To obtain the vessel binary image several alternatives method can be use from morphological to multi-resolution analysis methods. We use the typical edge detection Canny algorithm with local threshold. The results of the vessel edge detection are shown in Fig. 15.

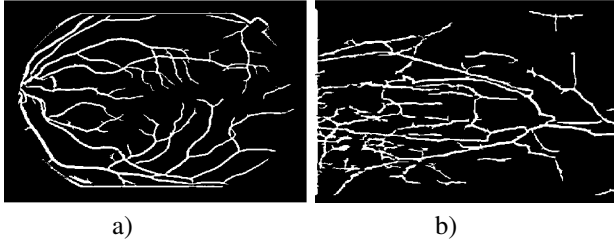


Fig. 15. Vessel edge detection of Retina-1 (a) and Conjunctiva-1 (b) images.

2) *Extraction of geometrical features:* For each vessels line we specify vessel bifurcations characteristic points and cross points of vessel intersections characteristic points, used information derived from connected number of point p . When $p = 1$, the connected number N_c of p is defined by the next equation

$$N_C^4 = \sum_{k \in S} (p_k - p_k p_{k+1} p_{k+2}) \quad (29)$$

$$N_C^8 = \sum_{k \in S} (\bar{p}_k - \bar{p}_k \bar{p}_{k+1} \bar{p}_{k+2}) \quad (30)$$

where: $S = (1, 3, 5, 7)$ and \bar{p} means $(1 - p)$.

Topological properties of the pixel p are shown in Table 1.

TABLE II
TOPOLOGICAL PROPERTIES OF p

THE VALUE OF N_C^4 OR N_C^8	3	4
PROPERTY OF PIXEL p	Branch	Cross

The feature vector corresponding to vessel topology and consecutively the number of bifurcations and cross points are stored in the feature vector. Moreover, the coordinates of all the extracted characteristic points are stored. The feature vector for each vessels consists of the following parts: - 2 numbers corresponding to the number of bifurcation points and cross points in each vessels, - subvector in which the coordinates of the bifurcation points are stored, - subvector in which the coordinates of the cross points are stored.

The correspondence between the vessel in an image and the vessel templates is based on the similarity between their characteristic points. The characteristic points are computed for each vessel template. The characteristic points of the vessel image are then compared with the characteristic points of each vessel template. Using the correspondence between the vessel characteristic points and vessel template characteristic points, we can calculate the total number of matching points and obtain the matching results. The process is illustrated in Figure 17.

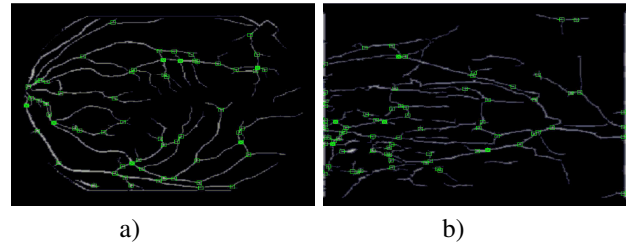


Fig. 16. Geometrical features of Retina-1 (a) and Conjunctiva-1 (b) images.

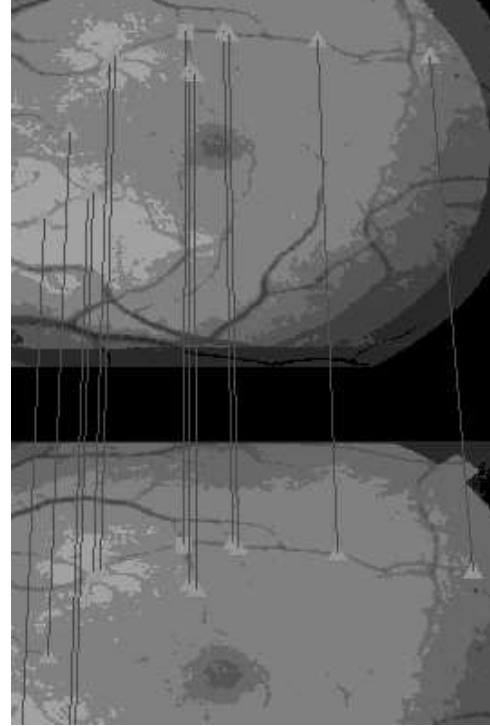


Fig. 17. The correspondence between the vessel characteristic points in retina image

3) *Texture feature from Gabor filters:* We use a bank of filters built from the real part of Gabor expression called as even-symmetric Gabor filter.

Gabor filtered output of the image is obtained by the convolution of the image with Gabor function for each of the orientation/spatial frequency (scale) orientation. The normalized retina or conjunctiva images are divided into blocks (Fig. 18). The size of each block in our application is $k \times l$ ($k = l = 20$). Each block (Fig. 19) is filtered with equation (31).

Given an image $f(x, y)$

$$G(x, y) = \sum_k \sum_l f(x - k, y - l) * Gab_{even}(x, y, W, \theta) \quad (31)$$

Features based on the Gabor filters responses can be represented by

$$\mu(x, y) = \frac{1}{XY} \sum_{x=1}^X \sum_{y=1}^Y G(x, y) \quad (32)$$

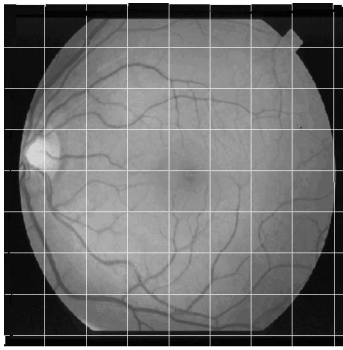
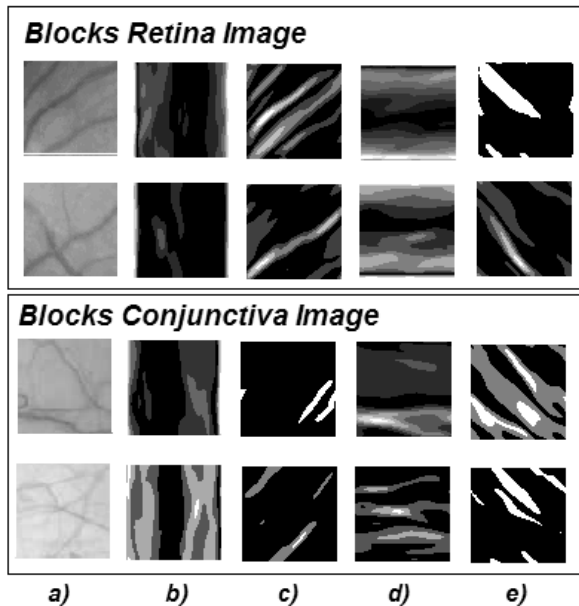


Fig. 18. Original block retinal images

Fig. 19. Original block retina image (a) and real part of $Gab(x; y; \theta_i)$ for $\theta = 0$ (b), $\theta = 45$ (c), $\theta = 90$ (d), $\theta = 135$ (e)

$$std(x, y) = \sqrt{\sum_{x=1}^X \sum_{y=1}^Y (|G(x, y)| - \mu(x, y))^2} \quad (33)$$

$$Skew = \frac{1}{XY} \sum_{x=1}^X \sum_{y=1}^Y \left(\frac{G(x, y) - \mu(x, y)}{std(x, y)} \right)^3 \quad (34)$$

where X, Y is image dimension.

The feature vector is constructed using $\mu(x, y)$, $std(x, y)$ and $Skew$ as feature components.

V. CONCLUSIONS

The main contributions of this work are the identification of the problems existing in biometrics systems - describing image feature extraction. We have described a possible approach to mapping biometric image into low-level features. This paper investigated the use of a number of texture features for biometrics systems.

REFERENCES

- [1] A.F. Abate, M. Nappi, D. Riccio, G. Sabatino. "2D and 3D face recognition: A survey," *Pattern Recognition Letters*, 28(14), pp. 1885-1906, 2007.
- [2] A. Abaza, A. Ross, C. Herbert, M.A.F. Harrison, M. Nixon, "A survey on ear biometrics", *ACM Comput. Surv.*, 45 (2) pp. 22:01-22:35, 2013.
- [3] W.W. Boles, B. Boashash, "A human identification technique using images of the iris and wavelet transform," *IEEE Transactions on Signal Processing*, 46, pp. 1185-1188, 1998.
- [4] K.W. Bowyer, K. Hollingsworth, P.J. Flynn, "Image understanding for iris biometrics: A survey", *Computer Vision and Image Understanding*, 110(2): pp. 281307, 2008.
- [5] M. Choras, "Image Feature Extraction Methods for Ear Biometrics A Survey", *6th International Conference on Computer Information Systems and Industrial Management Applications, CISIM '07*, pp. 261-265, 2007.
- [6] R.S. Choras, "Image Feature Extraction Techniques and Their Applications for CBIR and Biometrics Systems", *International Journal of Biology and Biomedical Engineering*, Issue 1, vol.1, pp. 6-16, 2007.
- [7] R.S. Choras, "Iris Recognition", *Computer Recognition Systems 3, AISC 57*, pp. 637-644, Springer-Verlag Berlin Heidelberg 2009.
- [8] R.S. Choras, "Iris-based person identification using Gabor wavelets and moments", *Proceedings 2009 International Conference on Biometrics and Kansei Engineering ICBACE 2009*, pp. 55-59, 2009.
- [9] J.G. Daugman, "Complete discrete 2-D Gabor transforms by neural networks for image analysis and compression," *IEEE Trans. Acoust., Speech, Signal Processing*, 36, pp. 1169-1179, 1988.
- [10] J.G. Daugman, "High confidence visual recognition of persons by a test of statistical independence," *IEEE Transactions on Pattern Analysis and Machine Intelligence*, 25, pp. 1148-1161, 1993.
- [11] J.G. Daugman, "Biometric personal identification system based on iris analysis", U.S. Patent 5 291 560, 1994.
- [12] N. Duta, "A survey of biometric technology based on hand shape", *Pattern Recogn.*, 42 (11), pp. 2797-2806, 2009.
- [13] D. Gabor, "Theory of communication," *J. Inst. Elect. Eng.*, 93, pp. 429-459, 1946.
- [14] R.M. Haralick, "Statistical and structural approaches to texture", *IEEE Transaction on Systems, Man and Cybernetics*, vol. 67, pp. 786-804, 1979
- [15] R. Haralick, K. Shanmugam, I. Dinstein, "Textural features for image classification", *IEEE Trans. on Systems, Man, and Cybernetics*, SMC-3(6):610-621, 1973.
- [16] L. Hong, *Automatic personal identification using fingerprints*, PhD thesis, Michigan State University, 1998.
- [17] J. Huang, L. Ma, Y. Wang, and T. Tan, "Iris recognition based on local orientation description", in *Proc. 6th Asian Conf. Computer Vision*, vol. II, pp. 954-959, 2004.
- [18] A.K. Jain, R.M. Bolle, S. Pankanti (eds.), *Biometrics: Personal Identification in Networked Society*, Norwell, MA: Kluwer, 1999.
- [19] A.K. Jain, P.J. Flynn, A. Ross, (eds.), *Handbook of biometrics*, New York: Springer, 2007.
- [20] C. Kirbas, K. Quek, "Vessel extraction techniques and algorithm: a survey", *Proceedings of the 3rd IEEE Symposium on Bioinformatics and Bioengineering (BIBE 03)*, 2003.
- [21] A. Kumar, C. Wu, "Automated human identification using ear imaging", *Pattern Recogn.*, 45(3), pp. 956-968, 2012.
- [22] A. Kumar, "Incorporating cohort information for reliable palmprint authentication", *Proceeding of ICVGIP*, , Bhubaneswar, pp. 583-590, 2008.
- [23] H.C. Lee, R.E. Gaensslen, *Advances in fingerprint technology*, Boca Raton: CRC Press, 2001.
- [24] C. J. Liu and H. Wechsler, "Gabor feature based classification using the enhanced Fisher linear discriminant model for face recognition", *IEEE Transactions on Image Processing*, vol. 11, no. 4, pp. 467- 476, 2002.
- [25] D. H. Liu, K. M. Lam, and L. S. Shen, "Optimal sampling of Gabor features for face recognition", *Pattern Recognition Letters*, vol.25, no.2, pp. 267-276, 2004.
- [26] L. Ma, Y. Wang, and T. Tan, "Iris recognition using circular symmetric filters", in *Proceedings of the 16th International Conference on Pattern Recognition*, vol. 2, pp. 414-417, 2002.
- [27] L. Ma, Y. Wang, and T. Tan, "Iris recognition based on multichannel Gabor filtering", in *Proc. 5th Asian Conf. Computer Vision*, vol. I, pp. 279-283, 2002.
- [28] L. Ma, T. Tan, Y. Wang, and D. Zhang, Personal identification based on iris texture analysis, *IEEE Transactions on Pattern Analysis and Machine Intelligence*, vol. 25, no. 12, pp. 1519-1533, 2003.

- [29] L. Ma, T. Tan, D. Zhang, and Y. Wang, "Local intensity variation analysis for iris recognition", *Pattern Recognition*, vol. 37, no. 6, pp. 1287-1298, 2005.
- [30] X. Meng, Y. Yin, G. Yang, X. Xi, "Retinal Identification Based on an Improved Circular Gabor Filter and Scale Invariant Feature Transform", *Sensors*, 13, pp. 9248-9266, 2013
- [31] M. Nixon, T. Tan, R. Chellappa, *Human Identification Based on Gait*, Springer, 2006 .
- [32] U. Park, R. Jillela, A. Ross, A. Jain, "Periocular biometrics in the visible spectrum", *IEEE Trans. Inform. Forensics Secur.*, 6 (1), pp. 96-106, 2011.
- [33] C. Park, J. Lee, M. Smith, and K. Park, "Iris-based personal authentication using a normalized directional energy feature", in *Proc. 4th Int. Conf. Audio- and Video-Based Biometric Person Authentication*, pp. 224-232, 2003.
- [34] H. Proenca and L. A. Alexandre, "UBIRIS: A noisy iris image database", *Proc. 13th International Conference on Image Analysis and Processing (ICIAP2005)*, pp. 970-977, 2005.
- [35] H. Proenca and L. A. Alexandre, "Iris segmentation methodology for non-cooperative iris recognition", *IEE Proc. Vision, Image & Signal Processing*, vol. 153, issue 2, pp. 199-205, 2006.
- [36] A. Ross, K. Nandakumar, A.K. Jain, *Handbook of Multibiometrics*, Springer, 2006 .
- [37] R. Sanchez-Reillo and C. Sanchez-Avila, "Iris recognition with lowtemplate size", in *Proc. Int. Conf. Audio- and Video-Based Biometric Person Authentication*, pp. 324-329, 2001.
- [38] Z. Sun, Y. Wang, T. Tan, J. Cui, "Improving iris recognition accuracy via cascaded classifiers", *IEEE Trans. on Systems, Man, and Cybernetics-Part C*, vol.35, no.3, pp.435-441, 2005.
- [39] T.N. Tan, "Rotation invariant texture features and their use in automatic script identification", *IEEE Trans. on PAMI*, 20(7):751-756, 1998.
- [40] C. Tisse, L. Martin, L. Torres, M. Robert, "Person identification technique using human iris recognition", in *Proc. Vision Interface*, pp. 294-299, 2002.
- [41] Y. Wang, J. Hu, D. Phillips, "A fingerprint orientation model based on 2d fourier expansion (FOMFE) and its application to singular-point detection and fingerprint indexing", *IEEE Transactions on Pattern Analysis and Machine Intelligence*, 29(4), pp. 573-585, 2007.
- [42] R.P. Wildes, J.C. Asmuth, G.L. Green, S.C. Hsu, R.J. Kolczynski, J.R. Matey, and S.E. McBride, "A machine vision system for iris recognition", *Mach. Vision Applicat.*, vol. 9, pp. 1-8, 1996.
- [43] R.P. Wildes, "Iris recognition: an emerging biometric technology", *Proceedings of the IEEE*, vol. 85, no.9, pp. 1348-1363, 1997.
- [44] J. Wright, A. Yang, A. Ganesh, S. Sastry, Y. Ma, "Robust face recognition via sparse representation", *IEEE Transactions on Pattern Analysis and Machine Intelligence*, 31(2), pp. 210-227, 2009.
- [45] D. Woodard, S. Pundlik, J. Lyle, P. Miller, "Periocular region appearance cues for biometric identification," *Computer Vision and Pattern Recognition Workshops (CVPRW)*, June 2010, pp. 162 -169.
- [46] G. Yang, X. Xi, Y. Yin, "Finger Vein Recognition Based on a Personalized Best Bit Map", *Sensors*, 12, pp. 1738-1757, 2012
- [47] S. Yoon, J. Feng, A. Jain, "Latent fingerprint enhancement via robust orientation field estimation", *International Joint Conference on Biometrics (IJCB)*, pp. 1-8, 2011.
- [48] X. Yuan and P. Shi, "A non-linear normalization model for iris recognition", *Proceedings of the International Workshop on Biometric Recognition Systems IWBRIS 2005*, pp. 135-142, China, 2005.
- [49] A. Yuksel, L. Akarun, B. Sankur, "Biometric identification through hand vein patterns", *International Workshop in Emerging Techniques and Challenges for Hand-Based Biometrics (ETCHB)*, pp.1-6, 2010.
- [50] L. Xueyan, G. Shuxu, G. Fengli, L. Ye, "Vein pattern recognitions by moment invariants", *Proceedings of the First International Conference on Bioinformatics and Biomedical Engineering*, 2007. pp. 612-615, 2007.
- [51] D. Zhang, W.K. Kong, J. You, et al., "Online palmprint identification", *IEEE Transactions on Pattern Analysis and Machine Intelligence*, 25(9), pp. 1041-1050, 2003.
- [52] W. Zhao, R. Chellappa, P.J. Phillips, A. Rosenfeld, "Face recognition: a literature survey", *ACM Computing Surveys*, 35, pp. 399-458, 2003.